

Asymmetric Hydrogenation Catalysis. X-ray Structural and Catalytic Studies of the Rhodium(I) Complex with (*R*)-Cycphos

Joel D. Oliver* and Dennis P. Riley

The Procter & Gamble Company, Miami Valley Laboratories, Cincinnati, Ohio 45247

Received November 30, 1982

The relative rates of reduction of various substrates with the previously reported Rh(I) complex of the chiral phosphine ligand (*R*)-1,2-bis(diphenylphosphino)-1-cyclohexylethane ((*R*)-Cycphos) are reported here and are compared to rates observed with other catalysts in its class. These studies reveal that this ligand affords not only high optical yields but also relatively fast chemical rates. The origins of these effects are interpreted in terms of a high degree of flexibility in the ligand which gives fast rates and a fixed chelate ring conformation that affords high optical yields. Crystal and molecular structural data are reported for two different polymorphs of the [Rh((*R*)-Cycphos)(norbornadiene)]ClO₄ (1) complex. The structures reveal distinctly different orientations of the phenyl and cyclohexyl rings of the cations (two independent cations in polymorph I and one in polymorph II). The cations are square planar, with Rh-C bond lengths ranging from 2.03 (3) to 2.28 (3) Å. The average of the Rh-P bond lengths is 2.29 (2) Å. The average P-Rh-P bond angle is 84.1 (6)°. The five-atom chelate rings of the three crystallographically independent cations adopt non-planar conformations with unique conformational angles. The structures are compared to other structures of Rh(I) complexes with chiral, chelating ligands. A systematic evaluation of the orientations of the aryl rings shows the structures do not obey the "edge-face" relation. Crystals of polymorph I at -100 °C are monoclinic of space group P₂₁ (No. 4) with *a* = 18.666 (13) Å, *b* = 9.510 (5) Å, *c* = 20.700 (15) Å, β = 103.93 (6)°, and *Z* = 4. Crystals of polymorph II at -85 °C are monoclinic of space group P₂₁ (No. 4) with *a* = 8.770 (4) Å, *b* = 17.877 (7) Å, *c* = 11.388 (5) Å, β = 96.15 (4)°, and *Z* = 2. Least-squares refinement of the structures has resulted in *R* = 0.083 (*R*_w = 0.081) based on 1795 unique reflections with *I* ≥ 2.5σ(*I*) for polymorph I and *R* = 0.051 (*R*_w = 0.039) based on 2328 reflections with *I* ≥ 2σ(*I*) for polymorph II.

Introduction

In recent years there has been a profusion of published work dealing with the design, synthesis, and use of chiral bidentate phosphines (cf. Figure 1) as ligands for Rh(I)-based asymmetric hydrogenation catalysts.¹ While the elegant work of the Halpern² and Brown³ groups has led to an understanding of many of the intimate mechanistic details of such asymmetric hydrogenation catalysts, much less work has been published detailing the effects the phosphine ligand structures have on the overall reaction rates and, of course, on optical yields. On the basis of the work of Halpern et al.,² we know that the mechanism shown in Figure 2 is operative.

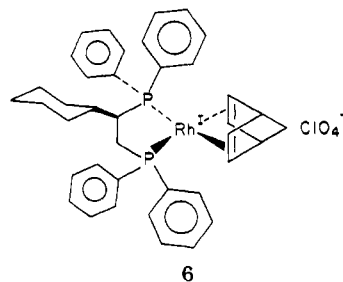
From that work, it has been found that the rate-determining step for this process is the oxidative addition of H₂ to the square-planar rhodium(I) enamide phosphine complex. Also, it is the *less favored* four-coordinate diastereomer which reacts faster with H₂. In other words, the origin of optical selectivity is due to rate differences in the subsequent steps along the sequence for the diastereomeric substrate adducts, not in an original preferred mode of

prochiral olefin-chiral catalyst binding.²

Another aspect that has become clear is that more stereochemically rigid complexes give better optical yields. This is believed to be due to the fact that a rigid arrangement of the bulky substituents around the metal center prevents any significant change in the asymmetric environment during the course of a catalytic cycle. As might be expected, very rigid chiral phosphines give very high optical yields. But, in general, these same ligands exhibit much slower rates than do the less hindered phosphines such as diphos (1a) or propfos (1b). From an inspection of the mechanism, it is reasonable to attribute this to the ease of reorganization of the coordination geometry about the metal upon addition of H₂ to the square-planar prochiral (olefin)rhodium phosphine complex. Consequently, chiral phosphines (from the class that owes its utility to a fixed chelate ring conformation about the metal (Figure 1)) may show very pronounced rate effects.

The results of rate studies in a variety of solvents for both the (*R*)-Cycphos (1d) and (*R*)-Propfos (1b) based catalysts are reported here. These rates are also compared to rates observed with other catalysts from this class of rhodium phosphine (Figure 1) complexes.

In addition to studying the hydrogenation rates, we undertook a crystallographic study of the catalyst precursor complex [Rh((*R*)-Cycphos)(norbornadiene)]ClO₄, 6, in order to determine if there were any subtle structural

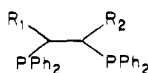


features that could be correlated to the optical yield and

(1) Inter alia: (a) MacNeil, P. R.; Roberts, N. K.; Bosnich, B. *J. Am. Chem. Soc.* 1981, 103, 2273. (b) Meyer, D.; Poulin, J.-C.; Kagan, H. B.; Levine-Pinto, H.; Morgat, J. L.; Fromageot, P. *J. Org. Chem.* 1980, 45, 4680. (c) Miyashita, A.; Yasuda, A.; Takaya, H.; Toriumi, K.; Ito, T.; Souchi, T.; Noyori, R. *J. Am. Chem. Soc.* 1980, 102, 7932. (d) Samuel, O.; Couffignal, R.; Laver, M.; Zhang, S. Y.; Kagan, H. B. *Nouv. J. Chim.* 1981, 5, 15. (e) Ojima, I.; Kogure, T.; Yoda, N. *J. Org. Chem.* 1981, 45, 4728. (f) Kashiwbara, K.; Hanoli, K.; Fujita, J. *Bull. Chem. Soc. Jpn.* 1980, 53, 2275. (g) Valentine, D., J.; Sun, R. C.; Toth, K. *J. Org. Chem.* 1980, 45, 3703; cf. preceding papers. (h) Koenig, K. E.; Bachman, G. L.; Vineyard, B. D. *Ibid.* 1980, 45, 2362. (i) Riley, D. P.; Shumate, R. S. *Ibid.* 1980, 45, 5187. (j) King, R. B.; Bakos, J.; Hoff, C. D.; Marko, L. *Ibid.* 1979, 10, 1729.

(2) Halpern, J. *Science (Washington, D. C.)* 1982, 217, 401 and references contained therein.

(3) (a) Brown, J. M.; Chaloner, P. A. *J. Am. Chem. Soc.* 1980, 102, 3040. (b) Brown, J. M.; Chaloner, P. A. *J. Chem. Soc., Chem. Commun.* 1980, 344. (c) Brown, J. M.; Chaloner, P. A.; Parker, D.; Descotes, G.; Lafont, D.; Sinou, D. *Nouv. J. Chim.* 1981, 5, 167. (d) Brown, J. M.; Murrer, B. A. *Tetrahedron Lett.* 1979, 4859. (e) Brown, J. M.; Chaloner, P. A.; Kent, A. G.; Murrer, B. A.; Nicholson, P. N.; Parker, D.; Sidebottom, P. J. *J. Organomet. Chem.* 1981, 216, 263. (f) Brown, J. M.; Murrer, B. A. *J. Chem. Soc., Perkin Trans. 2* 1982, 489.



- 1a, $R_1 = R_2 = H$, diphos
 b, $R_1 = CH_3$, $R_2 = H$, Propfos
 c, $R_1 = R_2 = CH_3$, Chiraphos
 d, $R_1 = C_6H_{11}$, $R_2 = H$, Cycphos
 e, $R_1 = R_2 = 1,3$ -cyclopentadiyl, Norphos
 f, $R_1 = R_2 = 1$ -methyl-4-isopropyl-cyclohex-1-ene-3,6-diyl, Phellanphos
 g, $R_1 = H$, $R_2 = \text{phenyl}$, Phenphos

Figure 1. Chiral, bidentate phosphine ligands capable of forming a five-membered chelate ring.

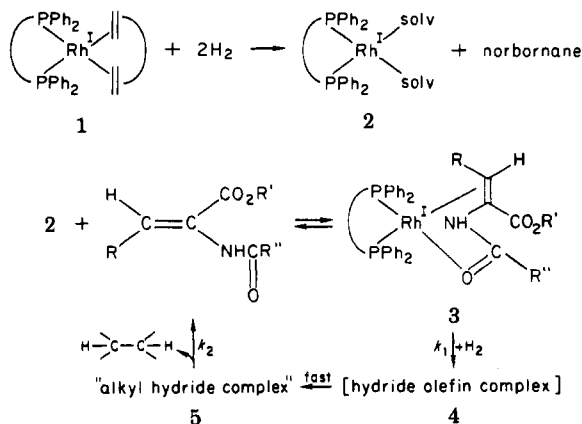


Figure 2. Mechanism of asymmetric hydrogenation of enamide substrates by chiral, bidentate phosphine Rh(I) complexes.

rate differences. The molecular structure of **6** has been compared to other published structures of chiral Rh(I) complexes in an attempt to identify essential structural features. Also, the crystallographic results are discussed in more general terms as they relate to the mechanism of asymmetric hydrogenations employing chiral, bidentate ligands complexed to Rh(I).

Experimental Section

Instrumentation. All optical rotations were obtained at 589 and 546 nm on a Rudolph Autopol III automatic polarimeter. X-ray measurements were performed on a Syntex P2₁ autodiffractometer with monochromated Mo K α radiation.

Syntheses. [Rh(*R*)-Cycphos](NBD)ClO₄, **6**. This complex was prepared by an adaptation of the method of ref 1i. In a typical preparation, 1.0 g of the dimer [Rh(NBD)Cl]₂ was dissolved in acetone under N₂ and 0.9 g of AgClO₄ added. The AgCl was removed by filtration, and the phosphine (2.05 g) was added slowly. The volume of acetone was reduced to 15 mL, and the solution was filtered through Celite. While the solution was hot, 20 mL of EtOAc was added slowly. Upon cooling by removal of acetone under vacuum, an orange precipitate formed. This was collected by filtration, washed with Et₂O, and dried in vacuo. The total yield was 2.4 g (74% yield based on starting Rh). Anal. Calcd for C₃₆H₄₂ClP₂O₄Rh: C, 63.02; H, 5.70; P, 4.17. Found: C, 63.29; H, 5.50; P, 4.01.

Crystals suitable for X-ray diffraction purposes were grown in two ways. Polymorph I was made by dissolving 0.5 g of complex **6** in 5 mL of warm CH₂Cl₂ under N₂. The resultant solution was then stored under N₂ for several weeks at 25 °C, whereupon deep dark red plates were obtained. Polymorph II was made by dissolving (under N₂) 0.5 g of complex **6** in 5 mL of warm CH₂Cl₂ and then adding dropwise Et₂O until slightly cloudy. This solution was allowed to sit undisturbed for several days, whereupon deep dark red plates were obtained.

Hydrogenation Procedure. A description of the methods for performing the catalytic reductions and for carrying out product workups has been reported previously.¹¹

The kinetic results were obtained on a standard constant pressure hydrogen uptake apparatus. The moles of hydrogen consumed could then be followed with time by measuring the

Table I. Summary of Crystal Data and Details of Data Collection

	I	II
Crystal Data		
formula	C ₃₆ H ₄₂ O ₄ ClP ₂ Rh	C ₃₆ H ₄₂ O ₄ ClP ₂ Rh
fw	775.1	775.1
<i>a</i> , Å	18.666 (13) ^a	8.770 (4) ^a
<i>b</i> , Å	9.510 (5)	17.877 (7)
<i>c</i> , Å	20.700 (15)	11.388 (5)
β , deg	103.93 (6)	96.15 (4)
<i>Z</i>	4	2
vol, Å ³	3566.3	1775.2
space group	P2 ₁	P2 ₁
<i>d</i> g cm ⁻³ (calcd)	1.44	1.45
<i>F</i> (000)	1600	800
<i>T</i> , °C	-100	-85
Data Collection		
cryst dimens, mm	0.15 × 0.20 × 0.25	0.07 × 0.14 × 0.30
μ (Mo K α), cm	6.73	6.76
limiting sphere	2 ≤ 2 θ ≤ 45	3 ≤ 2 θ ≤ 46
λ (Mo K α), Å	0.710 73	0.710 73
scan mode	θ -2 θ	θ -2 θ
scan rate, deg/min	variable, 4-29.3	variable, 4-29.3
reflectns measd	5389	2843
reflectns used	1795	2328
signif criterion, <i>I</i> ≥ <i>n</i> σ (<i>I</i>)	<i>n</i> = 2.5	<i>n</i> = 2
check reflectns ^b	(004), (020), (200)	(003), (020), (200), (111)
trans factor range	0.77-0.85	none applied

^a Cell constants were obtained from least-squares refinement of observed setting angles of 10 locally intense reflections for polymorph I and of 11 locally intense reflections for polymorph II. ^b Analysis of these intensities revealed only random variations (≤ 4% relative for polymorph I and ≤ 6% relative for polymorph II).

volume of H₂ consumed. The reported turnover numbers from these studies were calculated from the initial reaction rate constants which were themselves calculated from the first-order plots of log (mol of H₂) consumed vs. time.

Crystallographic Study of 6. For each polymorph a red, tablet-shaped crystal was mounted on a glass fiber and transferred to a Syntex P2₁ autodiffractometer, where it was maintained in a cold stream of dry N₂ gas using a Syntex LT-1 low-temperature attachment. The samples were maintained at reduced temperature for the duration of the diffraction experiments. The crystal data and details of data collection for both polymorphs are presented in Table I. The measured intensities for polymorph I were empirically corrected for absorption effects. For polymorph II no correction for absorption was applied to the intensity data.

The structures were solved by the heavy-atom method and were refined by full-matrix, least-squares techniques using the SHELXTL⁴ crystallographic software. The function minimized in the refinements was $\sum w(|F_o| - |F_d|)^2 / (m - n)$, where the weight $w = [\sigma^2(F_o) + g|F_o|^2]^{-1/2}$ and *g* is the ignorance factor (*g* = 0.0008 for polymorph I and *g* = 0.0003 for polymorph II). Neutral atom scattering factors⁵ for Rh, Cl, P, O, C, and H were used in the refinement, and the real ($\Delta f'$) and imaginary ($\Delta f''$)⁵ corrections for anomalous dispersion for all atoms were included in the calculations.

For both structures the phenyl substituents were treated as rigid groups with fixed bond lengths (C-C = 1.395 Å and C-H = 0.96 Å) and bond angles (120°). The isotropic temperature factor of each phenyl C atom was allowed to vary independently, while that of each phenyl H atom was held fixed at ~1.2 times

(4) Sheldrick, G. M. "SHELXTL: A Minicomputer Package for Crystal Structure Determination", Nicolet XRD Division, 1981.

(5) Ibers, J. A.; Hamilton, W. C. "International Tables for X-ray Crystallography"; Kynoch Press: Birmingham, England, 1974; Vol. IV.

Table II. Atom Coordinates ($\times 10^4$) for [Rh(NBD)((*R*)-Cycphos)](ClO₄) Polymorph I

atom	x	y ^a	z	atom	x	y ^a	z
Rh(1)	3015 (2)	0	4405 (2)	C(46)	3122 (12)	350 (2)	4144 (10)
Rh(2)	1750 (2)	-72	7720 (2)	C(41)	3335 (12)	294 (2)	3597 (10)
P(1)	3191 (6)	101 (1)	3453 (5)	C(52)	3975 (9)	-93 (2)	2855 (10)
P(2)	1819 (5)	-17 (1)	3807 (5)	C(53)	4622 (9)	-161 (2)	2806 (10)
PP(1)	2839 (5)	-16 (1)	8448 (4)	C(54)	5306 (9)	-109 (2)	3151 (10)
PP(2)	1510 (5)	-195 (1)	8596 (5)	C(55)	5343 (9)	11 (2)	3546 (10)
Cl(1)	2424 (7)	461 (1)	6129 (6)	C(56)	4696 (9)	79 (2)	3596 (10)
Cl(2)	2410 (9)	677 (2)	1416 (7)	C(51)	4012 (9)	27 (2)	3250 (10)
O(1)	2011 (21)	540 (4)	5591 (18)	C(61)	2835 (13)	-95 (3)	9284 (12)
O(2)	1821 (19)	417 (4)	6438 (16)	C(62)	2369 (17)	-231 (3)	9152 (16)
O(3)	2770 (27)	369 (5)	5923 (23)	C(63)	2097 (16)	-47 (3)	6803 (14)
O(4)	2902 (18)	569 (3)	6520 (16)	C(64)	1682 (29)	72 (6)	6930 (23)
O(5)	2089 (18)	571 (3)	1745 (15)	C(65)	694 (25)	-63 (5)	7039 (21)
O(6)	2339 (20)	642 (4)	767 (17)	C(66)	997 (19)	-174 (4)	6832 (17)
O(7)	2827 (32)	781 (6)	1671 (26)	C(67)	812 (31)	67 (6)	6559 (26)
O(8)	1801 (29)	736 (5)	1381 (22)	C(68)	1496 (23)	-140 (4)	6389 (19)
C(1)	2375 (23)	87 (5)	2795 (20)	C(69)	957 (18)	-35 (4)	5973 (16)
C(2)	1759 (19)	77 (4)	3027 (16)	C(71)	3589 (14)	-95 (3)	9767 (12)
C(3)	4128 (18)	-57 (4)	4870 (15)	C(72)	4041 (18)	-226 (4)	9819 (17)
C(4)	3963 (16)	46 (3)	5090 (14)	C(73)	4759 (18)	-222 (4)	10305 (15)
C(5)	3043 (16)	-147 (3)	5274 (13)	C(74)	4700 (21)	-194 (4)	10972 (17)
C(6)	2966 (18)	-28 (4)	5489 (14)	C(75)	4316 (19)	-56 (4)	10956 (18)
C(7)	3928 (21)	-166 (4)	5416 (18)	C(76)	3549 (18)	-69 (4)	10459 (15)
C(8)	3713 (22)	48 (4)	5747 (19)	C(82)	3226 (11)	236 (2)	8023 (8)
C(9)	4173 (19)	-83 (4)	6028 (16)	C(83)	3382 (11)	379 (2)	8069 (8)
C(11)	2301 (20)	174 (4)	2136 (17)	C(84)	3400 (11)	451 (2)	8661 (8)
C(12)	2956 (19)	162 (4)	1788 (16)	C(85)	3263 (11)	379 (2)	9206 (8)
C(13)	2897 (21)	256 (4)	1182 (18)	C(86)	3107 (11)	236 (2)	9160 (8)
C(14)	2053 (23)	253 (5)	713 (22)	C(81)	3088 (11)	164 (2)	8569 (8)
C(15)	1458 (25)	261 (5)	1052 (22)	C(92)	3554 (10)	-217 (2)	7830 (10)
C(16)	1545 (18)	165 (4)	1620 (16)	C(93)	4175 (10)	-279 (2)	7688 (10)
C(22)	1435 (14)	-278 (3)	4166 (10)	C(94)	4867 (10)	-217 (2)	7912 (10)
C(23)	1276 (14)	-421 (3)	4067 (10)	C(95)	4938 (10)	-92 (2)	8277 (10)
C(24)	1234 (14)	-481 (4)	3445 (10)	C(96)	4317 (10)	-30 (2)	8420 (10)
C(25)	1351 (14)	-399 (4)	2923 (10)	C(91)	3625 (10)	-92 (2)	8196 (10)
C(26)	1511 (14)	-256 (3)	3022 (10)	C(102)	1029 (12)	-148 (2)	9738 (11)
C(21)	1552 (14)	-196 (3)	3643 (10)	C(103)	532 (12)	-88 (2)	10065 (11)
C(32)	1329 (11)	170 (3)	4588 (13)	C(104)	4 (12)	8 (2)	9731 (11)
C(33)	806 (11)	231 (3)	4883 (13)	C(105)	-27 (12)	43 (2)	9070 (11)
C(34)	85 (11)	180 (3)	4736 (13)	C(106)	469 (12)	-17 (2)	8744 (11)
C(35)	-114 (11)	68 (3)	4295 (13)	C(101)	998 (12)	-112 (2)	9078 (11)
C(36)	409 (11)	7 (3)	4001 (13)	C(112)	473 (13)	-410 (2)	8519 (11)
C(31)	1130 (11)	58 (3)	4147 (13)	C(113)	171 (13)	-542 (2)	8315 (11)
C(42)	3584 (12)	382 (2)	3159 (10)	C(114)	528 (13)	-632 (2)	7963 (11)
C(43)	3621 (12)	527 (2)	3269 (10)	C(115)	1187 (13)	-591 (2)	7814 (11)
C(44)	3408 (12)	583 (2)	3816 (10)	C(116)	1489 (13)	-459 (2)	8018 (11)
C(45)	3159 (12)	495 (2)	4254 (10)	C(111)	1132 (13)	-369 (2)	8370 (11)

^a y coordinates are presented ($\times 10^3$).

the temperature factor of the C atom to which it is bonded. For polymorph I only 33% of the measured reflections had significant intensities above background. Due to the limited data, the refinement of the nongroup atoms was performed by using anisotropic temperature factors for the Rh and P atoms only and isotropic temperature factors for the C, O, and Cl atoms. For polymorph II all the nongroup, non-hydrogen atoms were refined by using anisotropic thermal parameters. Difference electron density maps revealed the locations of most of the H atoms of the two structures. The non-phenyl H atoms were subsequently included in the refinement at their fixed, idealized locations. Each H atom was assigned an isotropic thermal parameter whose value was 1.2 times the equivalent isotropic thermal parameter of the C atom bonded to it.

At this point the structures were subjected to parallel refinements, one for each possible enantiomer, in an attempt to assign the absolute configurations of the cations. For polymorph I refinement of the *R* enantiomer produced $R = 0.0833$ and $R_w = 0.0809$ and refinement of the *S* enantiomer produced $R = 0.0836$ and $R_w = 0.0809$. For polymorph II refinement of the *R* enantiomer produced $R = 0.0508$ and $R_w = 0.0386$ and refinement of the *S* enantiomer produced $R = 0.0515$ and $R_w = 0.0389$. With use of the Hamilton⁶ *R* factor ratio test, the results for both

structures were insignificant at even the 95% confidence level. Thus, unambiguous assignment of the absolute stereochemistry of **6** was not possible by using the X-ray data for either polymorph. This factor does not present a significant problem since the synthesis of the (*R*)-Cycphos ligand¹¹ was accomplished by an accepted, stereospecific route. Final difference electron density maps revealed only small peaks ($<1 \text{ e } \text{\AA}^{-3}$ for polymorph I and $<0.55 \text{ e } \text{\AA}^{-3}$ for polymorph II) at chemically unreasonable positions. Final atomic coordinates are given in Tables II and III. Bond lengths, bond angles, thermal parameters, hydrogen atom parameters, and structure factor amplitudes, as $10|F_o|$ and $10|F_c|$ in electrons, have been deposited.

Results and Discussion

Asymmetric Hydrogenation Studies. In an earlier publication we reported that the (*R*)-Cycphos (**1d**) based Rh(I) catalyst system gives not only consistently high optical yields but fast chemical rates with prochiral olefin substrates.¹¹ In Table IV the observed chemical rates and optical yields are reported for several asymmetric hydrogenation runs with the (*R*)-Cycphos (**1d**) and (*R*)-Prophos (**1b**)⁷ based catalysts. In general, the Cycphos-based

(6) Hamilton, W. C. *Acta Crystallogr.* 1965, 18, 502.

(7) Fryzuk, M. D.; Bosnich, B. J. *J. Am. Chem. Soc.* 1978, 100, 5491.

Table III. Atom Coordinates ($\times 10^4$) for [Rh(NBD)(*R*-Cycphos)](ClO₄) Polymorph II

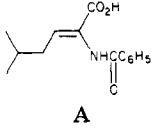
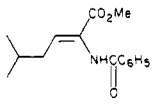
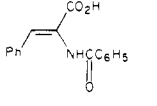
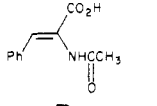
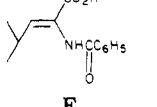
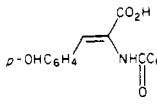
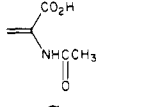
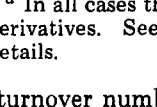
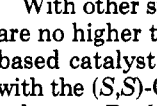
atom	x	y	z
Rh	6622 (1)	10000	7976 (1)
P(1)	7429 (3)	10660 (2)	6438 (2)
P(2)	6747 (4)	11150 (2)	8931 (2)
Cl	1543 (3)	9006 (2)	534 (3)
O(1)	1943 (10)	9774 (4)	514 (8)
O(2)	2863 (10)	8571 (4)	1001 (7)
O(3)	286 (11)	8900 (6)	1219 (9)
O(4)	1083 (11)	8777 (5)	-660 (8)
C(1)	7215 (12)	11690 (6)	6696 (8)
C(2)	7755 (11)	11802 (5)	8018 (8)
C(3)	5635 (12)	9023 (5)	7017 (9)
C(4)	7157 (13)	8880 (6)	7345 (10)
C(5)	7262 (13)	8474 (6)	8526 (10)
C(6)	6798 (14)	9113 (7)	9384 (9)
C(7)	5269 (14)	9253 (6)	9051 (9)
C(8)	4747 (12)	8721 (6)	8004 (9)
C(9)	5703 (14)	8036 (6)	8382 (10)
C(11)	8025 (12)	12233 (5)	5905 (8)
C(12)	7117 (13)	12962 (5)	5732 (9)
C(13)	7786 (14)	13506 (6)	4915 (11)
C(14)	9453 (15)	13666 (7)	5309 (11)
C(15)	10402 (13)	12945 (6)	5479 (9)
C(16)	9721 (11)	12417 (6)	6330 (9)
C(22)	3895 (7)	11221 (3)	9767 (5)
C(23)	2449 (7)	11519 (3)	9885 (5)
C(24)	1974 (7)	12173 (3)	9285 (5)
C(25)	2944 (7)	12529 (3)	8568 (5)
C(26)	4390 (7)	12231 (3)	8450 (5)
C(21)	4865 (7)	11577 (3)	9049 (5)
C(32)	7858 (7)	11997 (3)	10893 (6)
C(33)	8789 (7)	12134 (3)	11943 (6)
C(34)	9696 (7)	11563 (3)	12478 (6)
C(35)	9672 (7)	10854 (3)	11964 (6)
C(36)	8741 (7)	10716 (3)	10915 (6)
C(31)	7833 (7)	11288 (3)	10379 (6)
C(42)	10090 (7)	10639 (4)	5280 (4)
C(43)	11676 (7)	10607 (4)	5254 (4)
C(44)	12627 (7)	10427 (4)	6276 (4)
C(45)	11993 (7)	10279 (4)	7324 (4)
C(46)	10408 (7)	10310 (4)	7350 (4)
C(41)	9456 (7)	10490 (4)	6328 (4)
C(52)	5515 (8)	10987 (3)	4317 (6)
C(53)	4766 (8)	10789 (3)	3218 (6)
C(54)	4984 (8)	10079 (3)	2754 (6)
C(55)	5953 (8)	9568 (3)	3388 (6)
C(56)	6702 (8)	9766 (3)	4486 (6)
C(51)	6483 (8)	10476 (3)	4951 (6)

catalyst gives superior optical yields. These results confirm our earlier results and are not unexpected, since the bulkier cyclohexyl substituent favors the maintenance of a more fixed chelate ring conformation about the Rh and consequently a more fixed phenyl ring arrangement about the Rh atom.

The relative rates of hydrogenation with these catalysts show an interesting dependence on the solvent. In weakly coordinating solvents (MeOH, EtOAc) the Propfos-based catalyst consistently gives rates that are about twice as fast as those observed with the Cycphos-based catalyst system. In contrast to this, in the noncoordinating solvent dichloromethane the Cycphos-based catalyst gives faster rates than Propfos. In fact, with the 2-benzamido-5-methylhex-2-enoic acid (A) substrate, the fastest rates of asymmetric hydrogenation were observed with the (*R*)-Cycphos-based catalyst in CH₂Cl₂.

It is appropriate to compare our results with these two catalysts to the published rates for other chiral catalysts of this type (Figure 1). For example, with substrate F, the (*S,S*)-Chiraphos (1c) based catalyst⁸ was reported to have a turnover number of about $6 \times 10^{-4} \text{ s}^{-1}$ while the (*R*)-Cycphos-based catalyst was about $8.1 \times 10^{-3} \text{ s}^{-1}$. Similarly, with substrate G, the (*R*)-Cycphos-based catalyst gave a

Table IV. Observed Hydrogenation Rates under 1 atm H₂ Pressure and Optical Yields for Selected Chiral Rh(I) Catalysts^a

substrate	chiral phosphine	TN, mol/(s mol)	solv	opt yield, %
	(<i>R</i>)-Propfos	0.119	MeOH	86
	(<i>R</i>)-Propfos	0.164	EtOAc	88
	(<i>R</i>)-Propfos	0.044	CH ₂ Cl ₂	90
	(<i>R</i>)-Cycphos	0.065	EtOAc	96
	(<i>R</i>)-Cycphos	0.189	CH ₂ Cl ₂	95
	(<i>R</i>)-Cycphos	0.069	MeOH	94
	(<i>R</i>)-Cycphos	0.070	CH ₂ Cl ₂	84
	(<i>R</i>)-Cycphos	0.90	CH ₂ Cl ₂	90
	(<i>R</i>)-Cycphos	0.064	MeOH	88
	(<i>R</i>)-Cycphos	0.035	MeOH	93
	(<i>R</i>)-Phenphos		MeOH	84 ^{1j,3f}
	(<i>R</i>)-Phenphos	0.003 ¹⁰	EtOH	95
	(<i>R</i>)-Cycphos	0.37	MeOH	91
	(<i>R</i>)-Cycphos	0.081	MeOH	88
	(<i>R,R</i>)-Norphos	0.017 ⁹	MeOH	95
	Diphos	0.07 ⁹	MeOH	0
	Phellanphos	0.003 ¹⁰	EtOH	95
	(<i>R</i>)-Phenphos		MeOH	78 ^{1j,3f}
	(<i>R</i>)-Cycphos	0.37	MeOH	91
	(<i>R</i>)-Cycphos	0.0085	MeOH	98
	(<i>R</i>)-Propfos	0.012	MeOH	89
	(<i>R</i>)-Cycphos	0.21	MeOH	93
	(<i>R</i>)-Propfos	0.29	MeOH	89

^a In all cases the reduction products are (*S*)-amino acid derivatives. See ref 1i for more complete experimental details.

turnover number in MeOH of about 0.21 s^{-1} , while the (*S,S*)-Chiraphos-based catalyst was about 0.03 s^{-1} .⁸

With other sterically rigid phosphines, the optical yields are no higher than those observed with the (*R*)-Cycphos-based catalyst, but the rates are much less, as observed with the (*S,S*)-Chiraphos-based catalyst. For example with substrate D, the (*S,S*)-Norphos (1e) based catalyst⁹ gives a turnover number in MeOH of 0.017 s^{-1} ^{9a} compared to the fivefold rate increase observed with the (*R*)-Cycphos-based catalyst in MeOH. Similarly, the catalyst derived from an even more sterically rigid and constrained bidentate phosphine, Phellanphos (1f),¹⁰ gave much slower turnover numbers (0.003 s^{-1}) for substrate D than either the Cycphos or Norphos catalysts. Thus, within this group of chelating bidentate chiral phosphines, there appears to be an optimum structure. A combination of chelate ring

(8) Fryzuk, M. D.; Bosnich, B. J. *J. Am. Chem. Soc.* 1977, 99, 6262.

(9) (a) Kyba, E. P.; Davis, R. E.; Juri, P. N.; Shirley, K. R. *Inorg. Chem.* 1981, 20, 3616. (b) Brunner, H.; Pieronczyk, W. *Angew. Chem., Int. Ed. Engl.* 1979, 18, 620.

(10) Lauer, M.; Samuel, O.; Kagan, H. B. *J. Organomet. Chem.* 1979, 177, 309.

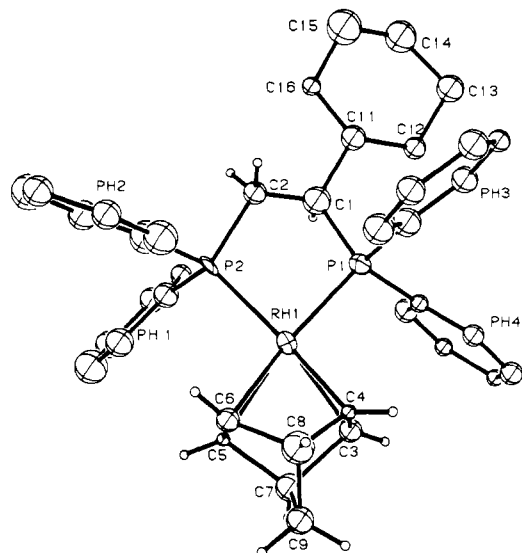


Figure 3. Perspective drawing of cation A of polymorph I indicating the atom labeling scheme. PH1, PH2, PH3, and PH4 contain the atoms C(21)–C(26), C(31)–C(36), C(41)–C(46), and C(51)–C(56), respectively.

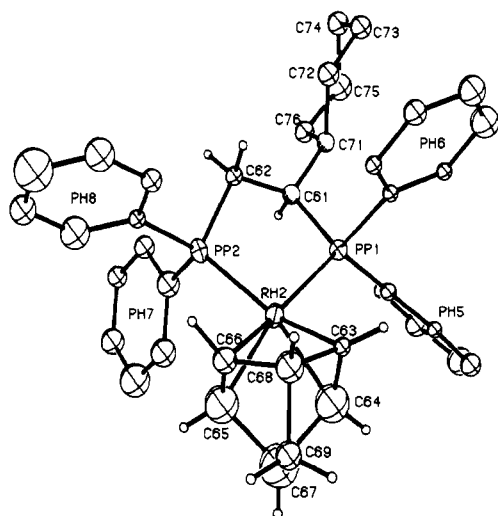


Figure 4. Perspective drawing of cation B of polymorph I indicating the atom labeling scheme. Atoms C61 and C71 have anomalously small thermal parameters and are drawn to an arbitrary size. PH5, PH6, PH7, and PH8 contain the atoms C(81)–C(86), C(91)–C(96), C(101)–C(106), and C(111)–C(116), respectively.

conformational rigidity giving good optical yields appears to be balanced against too rigid a structure that results in excessively slow rates of hydrogenation. Thus the optimum catalyst is one with a bulky R-group monosubstituted on the chelate ring and among these Cycphos appears to be the best.

Structural Studies. The structures of polymorphs I and II of **6** both consist of discrete cations and anions. Figure 3, 4, and 5 illustrate the stereochemistries of the three cations and indicate the superior quality of the X-ray diffraction data for polymorph II.

Each cyclohexyl ring assumes a chair conformation. The absolute values of the endocyclic torsion angles¹¹ range

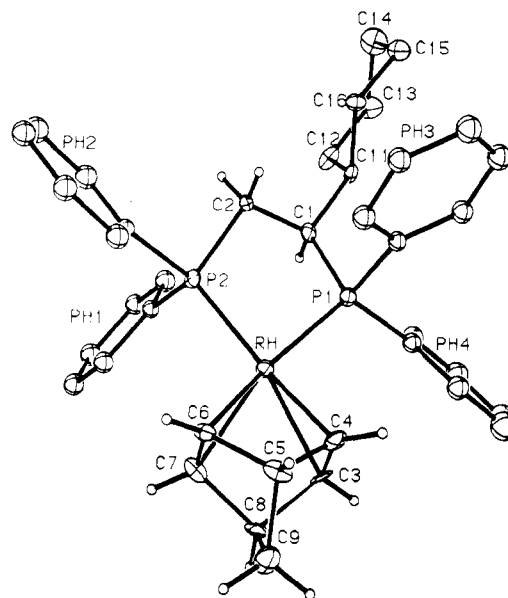


Figure 5. Perspective drawing of the cation of polymorph II indicating the atom labeling scheme. PH1, PH2, PH3, and PH4 contain the atoms C(21)–C(26), C(31)–C(36), C(41)–C(46), and C(51)–C(56), respectively.

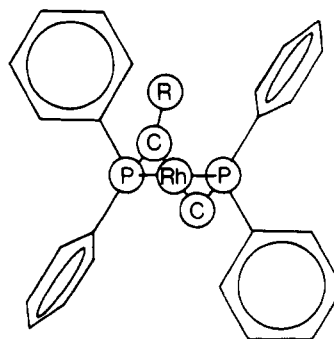


Figure 6. Schematic illustration showing the RhP_2 plane and the edge-face array of phenyl rings.

from 43 to 64° and have a mean value of 58 (3)° and 48 (4)° for cation A and cation B of polymorph I, respectively, and 55 (1)° for polymorph II. The average values of the C–C–C bond angles are 112 (4)° and 112 (1)° for polymorphs I and II, respectively. The C–C bond lengths have average values of 1.51 (6) and 1.52 (2) Å for the two polymorphs, respectively. These values compare favorably with those determined in other structures containing cyclohexyl substituents.

The generally accepted basis for the induction of chirality during the hydrogenation process is the chiral arrangement of the four phenyl groups occupying the pseudoaxial and -equatorial positions of a rather rigid chelate ring. The relative efficiencies of the catalysts generally increase as the chelate ring becomes more rigid. Thus bulkier substituents on the carbocyclic portion of the chelate ring produce more rigid chelate rings and thus improve the catalytic efficiency. The stereochemical features of Rh(I) complexes with various phenyl-substituted, bidentate ligands are described in Table V.

A systematic description of the chiral conformation of the phenyl substituents has been suggested by Knowles and co-workers¹⁶ which they term the edge-face arrange-

(11) Klyne, W.; Prelog, V. *Experientia* 1960, 16, 521.

(12) Ball, R. G.; Payne, N. C. *Inorg. Chem.* 1977, 16, 1187.

(13) Payne, N. C.; Stephan, D. W. *Inorg. Chem.* 1982, 21, 182.

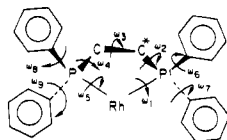
(14) Toriumi, K.; Ito, T.; Takaya, H.; Souchi, T.; Noyori, R. *Acta Crystallogr., Sect. B* 1982, B38, 807.

(15) Ball, R. G.; James, B. R.; Mahajan, D.; Trotter, J. *Inorg. Chem.* 1981, 20, 254.

Table V. Torsion Angles Defining the Stereochemistries of Chiral Rh(I) Complexes with Bidentate Ligands

compd	ω_1	ω_2	ω_3	ω_4	ω_5	ω_6	ω_7	ω_8	ω_9
6 ^a (cation A)	-8	26	-34	26	-7	-17	89	26	73
6 ^a (cation B) polymorph I	-3	31	-51	48	-22	-29	-69	51	32
6 ^a (polymorph II)	-14	42	-52	42	-11	-28	-70	6	67
7, ^b (NBD)Rh[(S,S)-Renorphos]	14	-47	64	-48	15	5	64	-45	-8
8, ^c (COD)Rh[(S,S)-Chiraphos]	15	-43	52	-41	12	9	-75	-75	10
9, ^d (NBD)Rh[(S)-Amars]	10	8		84	-50	-27	-76		
9, ^d (NBD)Rh[(S)-Amars]	8	6		78	-44	63	17		
10, ^e (TNBD)Rh[(S)-Binap]	-41	71		67	-35	55	6	4	4
11, ^f (H)Rh[(S,S)-Diop]	-52	70		38	15	-74	-34	79	14
11, ^f (H)Rh[(S,S)-Diop]	-43	64		60	-2	4	-70	37	50

^a This work. ^b Reference 9a. ^c Reference 12. ^d Reference 13 (six-atom chelate ring). ^e Reference 14 (seven-atom chelate ring). ^f Reference 15 (seven-atom chelate ring). The torsion angles are defined as



The angles ω_6 - ω_9 are Rh-P-C-C(phenyl) torsion angles. Of the two torsion angles for each phenyl ring, the value tabulated was chosen to lie in the interval $0 \leq |\omega| \leq 90^\circ$.

ment. An illustration of the idealized edge-face arrangement is shown in Figure 6. For catalysts which conform to this description, the four phenyl substituents are arranged about the metal atom in an alternating edge-face manner so that a phenyl substituent displaying an edge to the metal atom is adjacent to another phenyl group displaying a face to the metal atom.

The phenyl ring array thus should be face-edge-face-edge. Inspection of Figures 3, 4, and 5 shows the three cation geometries of 6 violate this general relationship. For cation A of polymorph I, the array is approximately edge-edge-face-face. For cation B of polymorph I, the phenyl rings PH(6), PH(7), and PH(8) have a disposition intermediate between edge and face, and phenyl ring PH(5) is facially disposed to Rh(2). For polymorph II, the phenyl ring array is approximately intermediate-edge-face-face. Figures 4 and 5 show also that these two cations have a virtually identical orientation of the cyclohexyl ring to the chelate ring. The chelate ring conformations in the cations are very similar and the phenyl ring orientations on P(1) and PP(1) are also very similar. The orientations of the phenyl rings on P(2) and PP(2) are quite dissimilar. Figures 3 and 5 show that cation A of polymorph I and the cation of polymorph II have dissimilar orientations of the cyclohexyl rings. They also have different orientations of the phenyl rings attached to P(1). The orientations of the phenyl rings on P(2), however, are very similar. These similarities and differences between cation geometries suggest the chelate ring conformation and the orientation of the phenyl rings on P(1) are locked by the orientation of the cyclohexyl ring. Further, the orientations of the phenyl rings bonded to P(2) appear to be sensitive to subtle intermolecular interactions.

This edge-face arrangement can be alternatively described in terms of the torsion angles about the P(chelate)-C(phenyl) bonds. A tabulation of these values and other metrical features of published chiral catalyst precursor structures is presented in Table V. The data in the table describing the orientations of the phenyl substituents are ω_6 , ω_7 , ω_8 , and ω_9 . A structure ideally conforming to the edge-face arrangement would have $|\omega_6| = |\omega_9| = 90^\circ$ and $\omega_7 = \omega_8 = 0^\circ$ or $\omega_6 = \omega_9 = 0^\circ$ and $|\omega_7| = |\omega_8| = 90^\circ$ for

structures with the opposite chirality of the five-atom chelate ring. A cursory inspection of these torsion angles shows that only the structure of the Rh(I) complex with (S,S)-Chiraphos¹² actually displays the edge-face arrangement. In fact, most of the phenyl groups are oriented midway between an edgewise and a facewise ($30^\circ \lesssim |\omega| \lesssim 75^\circ$) disposition. Additionally, the structural studies of 6 and the Rh(I) complexes of Diop (11)¹⁵ and Amars (9)¹³ show the conformational array of the four phenyl groups is flexible. The existence of different phenyl ring conformations in these similar Rh(I) catalyst precursors offers additional support to Halpern's argument² that the outcome of chiral hydrogenation is a kinetic consequence rather than purely an enantiofacial discrimination consequence.

The endocyclic torsion angles, ω_1 , ω_2 , ω_3 , ω_4 , and ω_5 , given in Table V analytically describe the conformation of the chelate rings. The signs of the torsion angles for 6, 7, and 8 show the chirality of the chelate ring is correlated to the chirality of the bidentate phosphine ligand. Thus 7^{9a} and 8¹² (with S,S absolute configuration) have torsion angles with magnitudes similar to those of 6 (with R absolute configuration) but with opposite signs. Comparison with the chelate conformations of 9, 10, and 11¹³⁻¹⁵ is less informative since these cations have six- or seven-atom chelate rings. For these compounds, the torsion angles defined by the Rh atom, P1, P2, and the C atoms attached to P1 or P2 are given in Table V.

In other published structures of Rh complexes with chiral, bidentate ligands the diene ligands are skewed with respect to the metal atom coordination plane. Thus the midpoints of the olefinic bonds do not lie in the coordination plane but rather lie on opposite sides of the plane. Kyba et al. have suggested the forces that result in the nonideal diene orientation may be responsible for the enantioselective hydrogenation of prochiral olefins.^{9a}

The norbornadienes are skewed in opposite senses for the two crystallographically unique cations of the Rh-(amars) complex, 9.¹³ For the published structures^{9a,12} of Rh(I) complexes with five-atom RhPCCP rings with S,S absolute stereochemistries, the diene ligands are rotated counterclockwise away from the idealized conformation with the olefinic bonds perpendicular to the coordination plane. The norbornadiene ligands of 6 are also skewed from their idealized orientation as indicated by the out-of-plane distances given in Table VI and the illustrations

(16) Knowles, W. S.; Vineyard, B. D.; Sabacky, M. J.; Stults, B. R. "Fundamental Research in Homogeneous Catalysis"; Tsutsui, M., Ed.; Plenum Press: New York, 1980; p 523 and references contained therein.

Table VI. Distances (Å) of Selected Atoms from the Coordination Plane

cation A		cation B		polymorph II	
Rh(1)	0	Rh(2)	0	Rh	0
P(1)	0	PP(1)	0	P(1)	0
P(2)	0	PP(2)	0	P(2)	0
C(3)	-0.70	C(63)	-0.90	C(3)	-0.75
C(4)	0.45	C(64)	0.52	C(4)	0.61
C(5)	-0.57	C(65)	0.50	C(5)	1.16
C(6)	0.66	C(66)	-0.81	C(6)	0.83
C(7)	-1.08	C(67)	0.99	C(7)	-0.54
C(8)	1.13	C(68)	-1.39	C(8)	-1.09
C(9)	-0.01	C(69)	-0.42	C(9)	0.01

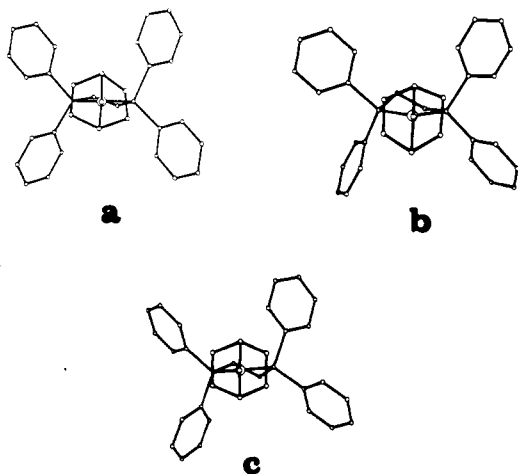


Figure 7. Orientation of the NBD ligands to the chelate planes: (a) cation A of polymorph I; (b) cation B of polymorph I; and (c) the cation of polymorph II. The view directions are from the NBD sides of the complexes.

shown in Figure 7. For cation A of polymorph I and the cation of polymorph II, the sense of the norbornadiene skewness is clockwise with respect to the coordination plane and thus agrees with the hypothesis that the sense of the skewness is due to the chirality of the catalyst pocket. This similarity between the cations is more remarkable since the orientations of the cyclohexyl groups on the chelate rings differ by a rotation of approximately 90° about the C(chelate)–C(cyclohexyl) bond which results in a different array of phenyl group orientations. The Rh–C bond lengths are also affected by the skewness of the NBD ligands of these cations. In each case the Rh–C bond lengths to the olefin trans to the phosphorus adjacent to the chiral carbon atom of the bidentate phosphine ligand are longer than those to the other olefin. The respective bond lengths are Rh(1)–C(5) = 2.27 (3) Å, Rh(1)–C(6) = 2.28 (3) Å, Rh–C(6) = 2.25 (1) Å, and Rh–C(7) = 2.24 (1) Å vs. Rh(1)–C(3) = 2.14 (3) Å, Rh(1)–C(4) = 2.03 (3) Å, Rh–C(3) = 2.19 (1) Å, and Rh–C(4) = 2.19 (1) Å. Although cation B of polymorph I and the cation of polymorph II have a very similar orientation of cyclohexyl rings, the dislocations of the diene ligands from their idealized orientation are distinctly different. The diene ligand of cation B is displaced out of the coordination plane

so the midpoint of the olefinic bonds and the bridging C atom C69 are each approximately 0.4 Å out of the coordination plane. This different sense of skewness is reflected in the Rh–C bond lengths. The Rh–C bond lengths for this cation are Rh(2)–C(63) = 2.16 (3) Å, Rh(2)–C(64) = 2.11 (5) Å, Rh(2)–C(65) = 2.13 (4) Å, and Rh–C(66) = 2.25 (3) Å. These bond lengths do not obey the relationship observed in the other crystallographically independent cations of 6. The orientation of the diene ligand thus appears to be sensitive to a variety of intermolecular and intramolecular forces for the two polymorphs of 6.

Conclusions

From our crystallographic results, we were surprised to find three unique cation geometries for 6. Since the [Rh(*R*)-Cycphos] system is an excellent catalyst giving high optical yields, we were also surprised to discover from the X-ray results that the complex 6 does not show the "edge–face–edge–face" conformational pattern of the *P*-aryl rings. Additionally, the crystallographic results reveal the conformation of the chelate ring in the [Rh(*R*)-Cycphos] moiety is *not* rigidly fixed. Although the cyclohexyl substituent is always equatorial, two different orientations of the cyclohexyl ring to the chelate ring were found. Also, other portions of the ligand show conformational flexibility. For example, the array of phenyl ring orientations observed for 6 suggests these rings are free to rotate *in solution*.

These results clearly show that this coordinated phosphine ligand does not form an absolutely rigid complex but that much flexibility and numerous rotational degrees of freedom are associated with the ligand backbone, as well as, with the *P*-phenyl rings. Such conclusions are also supported by the hydrogenation rate data observed with the (*R*)-Cycphos-based catalyst and with other catalysts of this class. Some flexibility in the coordinated chiral phosphine ligand is required for rapid hydrogenation rates. Furthermore, any predictions of catalyst efficiency based on the apparent rigidity of the chelate ring and the phenyl ring array, e.g., from a Drieding model, cannot alone account for the subtle dynamical features of the catalyst complex and should not be expected to give a complete description of the geometry of the catalyst/substrate interaction.

Acknowledgment. We wish to thank Mr. L. C. Strickland (of these laboratories) for his assistance with the X-ray structure investigations.

Registry No. 1b, 67884-32-6; 1e, 71042-54-1; 1f, 72021-47-7; 6, 85735-47-3; A, 75421-32-8; B, 75421-33-9; C, 26348-47-0; D, 55065-02-6; E, 64896-31-7; F, 64896-32-8; G, 5429-56-1; [Rh(NB-D)Cl]₂, 12257-42-0; AgClO₄, 7783-93-9; PhCH₂CH(CO₂H)NHCOC₆H₅, 2566-22-5; PhCH₂CH(CO₂H)NHCOC₆H₅, 1466-83-7; *p*-HOC₆H₄CH₂CH(CO₂H)NHCOC₆H₅, 2566-23-6; CH₃CH(CO₂H)NHCOC₆H₅, 97-69-8; (CH₃)₂CHCH₂CH₂CH(CO₂H)NHCOC₆H₅, 75421-34-0; (CH₃)₂CHCH₂CH₂CH(CO₂Me)NHCOC₆H₅, 75421-35-1.

Supplementary Material Available: Listings of anisotropic thermal parameters, H atom coordinates, bond lengths, bond angles, and structure factor amplitudes (34 pages). Ordering information is given on any current masthead page.